PORT SAID ENGINEERING RESEARCH JOURNAL
Faculty of Engineering - Port Said University
Volume 29 No. 3 pp: 142:156

5G Millimeter Wave High Isolation MIMO Antenna Arrays Based on Optimization

*Amany A. Megahed [1], Heba Y. M. Soliman [2, *]*

[1] *Electronic and Communication Department, Higher Institute of Engineering and Technology in New Damietta, Damietta, Egypt, email: engamany@yahoo.com*
[2] *Electronic and Communication Department, Faculty of Engineering, Port Said University, Port Fouad, Egypt, email: hebayms@eng.psu.edu.eg.*
**Corresponding author, DOI: 10.21608/pserj.2025.320488.1367*

Received 8-10-2024,
Revised 6-11-2024,
Accepted 12-5-2025

ABSTRACT

This work investigates a small, high-gain, two-port multiple-input, multiple-output (MIMO) antenna system. Each element of the MIMO array consists of two antennas connected by a 1:2 T-junction with 50Ω impedance matching to a single feed. In order to accommodate 5G millimeter wave applications, the antenna element uses the 26–40 GHz band, while the branching network's impedance within the element is matched to 100Ω. The gain and efficiency of radiation of the antenna element are set to 9dBi and 91%, respectively. The planned MIMO system has a value of roughly 93% efficiency and the gain is set to be approximately 10 dBi. The total length and width of the antenna array are 25.4, 15.45, 1.6 mm individually. FR-4 substrate is employed in the manufacturing process, which significantly lowers costs. Because of the decoupling surface between the antennas and their orthogonality, the antenna array has great isolation between elements. The simulated findings show that the measured mutual coupling (MC) value between the array members decreases by less than -30dB. It is enhanced to have an Envelope Correlation Coefficient (ECC) $< < 2\times10^{-4}$. Furthermore, there is an improvement of -30dB in the Total Active Reflection Coefficient (TARC), a reduction of less than 0.2 bits/sec/Hz in the Channel Loss Capacity (CCL), and a roughly 10dB Diversity Gain (DG) and Mean Effective Gain (MEG). Using CST Microwave Studio 2019, the suggested structure was created. Improved experimental findings are observed in relation to the simulation results, accordingly, the antennas are built and tested.

Keywords: Fifth Generation. Envelope Correlation Coefficient. Multiple Input Multiple Output. Mean Effective Gain. Total Affective Reflection Coefficient. Channel Capacity Loss.

1 INTRODUCTION

The technique of MIMO antennas is crucial for 5G wireless networks. Cost, energy, and spectrum efficiency are all improved by this technique. MIMO has been extensively utilized to greatly enhance channel capacity in a variety of systems. Owing to space constraints and aesthetic considerations, compact array antennas are frequently utilized. [1] presented a novel MIMO array design that operates within a bandwidth range of 3.2 to 4 GHz, achieving a notable gain of 2.5 dBi, thereby advancing the performance of communication systems in this frequency range. And [2] the authors introduced a 2-port U-Slot Patch array operating in the frequency range of 26.94 to 31.08 GHz, achieving a high gain of 13.1 dBi, and notably, without the use of decoupling surfaces demonstrating an efficient design that minimizes complexity while maintaining strong performance. In [3], the authors proposed a four-port MIMO system employing a variety of techniques to achieve high isolation between antenna ports, with the antenna dimensions measuring 46 mm × 46 mm × 1.6 mm^3. The system provides an isolation level of over 15 dB, with a peak gain of 9 dBi and an efficiency of 91%. The operating bandwidth spans from 3.2 to 5.7 GHz, offering

a versatile solution for mid-band communication systems. In [4], the authors utilized a Defected Ground Structure (DGS) between antennas to effectively reduce mutual coupling, thereby enhancing system performance in multi-antenna configurations. Meanwhile, [5] introduced a two-port MIMO antenna with an integrated isolating element designed to operate over a broad frequency range from 27 GHz to above 40 GHz, making it suitable for 5G millimeter-wave (MMW) applications. This design achieves a gain of 10 dBi and an impressive efficiency of 95%, highlighting its potential for high-performance wireless communication in the emerging 5G and beyond spectrum.

In [6], the authors presented a four-port MIMO array with compact dimensions of 30 × 35 × 0.76 mm^3. This array operates over a frequency range of 25.5 to 29.6 GHz and achieves a gain of 8.3 dBi, demonstrating its potential for use in mid-frequency 5G applications. In [7], a more advanced eight-port MIMO system was introduced, covering the frequency range from 27.5 to 29.5 GHz. This design employs the high-cost Rogers Duroid 5880 substrate, which enhances the system's performance but may limit cost-effectiveness in commercial applications. Meanwhile, [8] presents a dual-band antenna with four ports, designed to operate in the 5G millimeter-wave (MMW) frequency bands. The system achieves a remarkable isolation of 25 dB and a gain of approximately 5 dBi, providing a balanced trade-off between isolation and efficiency. In [9], a four-element MIMO antenna operating at both 28 and 38 GHz was realized, achieving a significant isolation of 30 dB and a gain of 9 dBi, highlighting its suitability for high-performance MMW communication. In [10], a substrate-integrated waveguide (SIW) antenna was proposed for a four-port MIMO configuration, operating within the 5G MMW frequency range. This design offers a gain greater than 5 dBi, showcasing its potential for integration in future MIMO-based communication systems. Numerous studies have explored various techniques to reduce mutual coupling in MIMO arrays. For example, electromagnetic bandgap (EBG) structures have been used effectively to mitigate coupling effects, as demonstrated in [11] and further explored in [12-13]. In [14], the authors proposed a meta-surface superstrate featuring a 4 × 4 array, designed with dimensions of 110 × 110 × 1.52 mm^3. The design uses RO4350B material as the substrate and operates at 5.8 GHz. This antenna achieves a gain of 5 dBi and an efficiency of 77%, making it suitable for applications requiring both compact size and efficient performance. In [3] and [15–16], the Neutralization Line (NL) approach was applied to reduce mutual coupling between antenna elements, enhancing the overall isolation and performance of the MIMO system. This technique has been widely used to improve antenna arrays' efficiency in multi-port configurations. Meanwhile, [3] and [17–18] introduced the Parasitic Element (PE) method, which further mitigates mutual coupling and optimizes antenna performance by integrating passive elements that interact with the main radiating elements. Certain studies, such as [8], do not employ isolating elements between antenna ports. For I stance, in [17], high isolation is achieved solely by leveraging the orthogonality between antenna elements, presenting a simpler design that avoids additional isolating structures. Additionally, recent research in mmWave antenna arrays has explored various techniques and applications to meet the demands of emerging wireless technologies, as demonstrated in [19–22], which present advancements in array configurations and performance improvements for mmWave and 5G systems.

Optimization techniques such as Genetic Algorithm (GA) [23–25], Artificial Neural Network (ANN), and Particle Swarm Optimization (PSO) [26–28] have found widespread applications in communication systems, particularly in optimizing antenna designs and system performance. In this paper, an orthogonal two-port MIMO array is proposed to mitigate the effects of mutual coupling, which is critical for improving the performance of multi-port antenna systems. The proposed antenna array is designed to support 5G mmWave applications, enabling higher data capacity and faster communication speeds to meet the demands of 5G wireless communication, high-speed data transmission, and the Internet of Things (IoT) devices. The antenna operates over a wide frequency range from 26 GHz to 40 GHz, providing the necessary bandwidth for these advanced applications. Constructed using an FR-4 substrate with a relative permittivity of 4.3, the design is optimized for cost-effectiveness and ease of manufacturing. Each antenna element is composed of two coupled elements, fed by a single 1:2 T-junction power divider with 50Ω impedance matching, as described in [29–31]. The overall size of the MIMO array is 25.4 mm × 15.45 mm with a thickness of 1.6 mm. The design achieves a gain of approximately 12 dBi and an efficiency of 95%, demonstrating its potential for high-performance wireless communication. In the field of antenna design, methods such as Genetic methods (GA) and Particle Swarm Optimization (PSO) are essential for enhancing antenna system performance and optimizing antenna parameters. These optimization methods are especially helpful when designing intricate antenna systems.

There are a lot of researchers [32-34] introduced the benefits of using PSO algorithm to optimize of antenna parameters such as dimensions, feed position, and shape to achieve desired radiation characteristics (e.g., gain, directivity, bandwidth), to optimize the shape and size of antennas, especially when considering complex geometries like fractal antennas or antennas with non-conventional designs, it can handle multi-objective optimization problems where multiple conflicting parameters (e.g., gain vs. bandwidth) need to be simultaneously optimized and also it can reduce computational costs and time, making it suitable for real-

time applications. Also, GA has a role in Antenna design [35-37]. GA is especially useful for exploring large and complex design spaces where the optimal solution is not easily attainable using traditional methods. It can be used to optimize both the geometry and topology of antennas, including irregular or fractal-shaped antennas. It is particularly effective in dealing with trade-offs in antenna design, such as between antenna size and radiation efficiency, or between bandwidth and gain. Since it does not require gradient information (unlike traditional optimization methods), it can handle non-differentiable, multimodal, and noisy objective functions commonly found in antenna design.

Among the various optimization techniques, PSO is chosen for its simplicity and efficiency, requiring few parameters for implementation. In the CST simulation environment, PSO is used to optimize the antenna's dimensions by iterating through initial parameter values and evaluating the fitness function until the desired performance specifications are met.

The remainder of the paper is organized as follows. In Section 2, describes the antenna element proposal. Section 3 describes the two-port MIMO antenna array design. Section 4 shows the results and discussion. Section 5 labels MIMO antenna evaluation. Finally, the conclusion is presented in Section 6.

2 ANTENNA ELEMENT DESIGN

Two optimization algorithms, Particle Swarm Optimization PSO and Genetic Algorithm GA are used for designing the antenna element.

2.1 Antenna Element using PSO

PSO is a computational approach that operates with the following steps for optimization (Fig. 1 (a)). The fundamental PSO algorithm works as follows:

- Take initial values for position and velocity from the solution space to begin solving the problem.
- Assess each particle's fitness and update the personal and global bests (gbest and Pbest).
- Refresh each particle's position and velocity.
- Repeat steps 1 through 3 until the requirement is satisfied. The spatial position of the i^{th} particle is considered to be Xi = (xi1, xi2, xi3, …xiD), where i = 1, 2,..., m. The position vector of each particle determines its fitness value, and the PSO algorithm iteratively seeks the best solution to evaluate the particle Xi.
- Each particle in the search area has a velocity of Vi = (vi1, vi2, vi3,... viD).
- Pi = (Pil, Pi2, Pi3, …, PiD) specifies the optimal location of the i^{th} particle, and the suitable fitness value Fi represents the suitable fitness value.
- The global best position can be defined as the particle's best location overall. Pg is equal to (Pgl, Pg2, Pg3, ..., PgD), and the global best fitness value Fg is the corresponding fitness value [26].

$$vid = wvid + c1r1\ (Pid - Xid) + c2r2\ (PgD - Xid) \quad (1)$$

$$xi(d+1) = xid + vid \quad (2)$$

The acceleration coefficients, c1 and c2, are two positive constants where w is the inertia weight and r1 and r2 are two random variables in the interval [0, 1]. Using Eq. (1), the particle's new velocity is determined by taking into account its best position, its previous velocity, and the group's best experience. Eq. (2) represents the position adjustment due to particle contact.

2.2 Antenna Element using GA

A search-based optimization system focused on the ideas of genetics and natural selection is called a genetic algorithm (GA). It is useful when a huge number of parameters is involved, and the search space is quite vast. The population of particle swarm optimization, in contrast to genetic algorithms, migrates to a better site without producing new particles as progeny. It was found that GA was a helpful tool for searching and optimization issues. The global optimum solution to a problem is not always found by GA, and long computations and iterations take a lot of time.

Here's how the fundamental genetic algorithm operates (Fig. 1 (b)):

- (Beginning) Genetic random population of n chromosomes.
- (Fitness) Analyze each chromosome x's fitness, f(x) inside the population.
- (New population) Start a new population by following the same procedures again until the new population is fully formed.
- (Selection) indicate two parent chromosomes from a population based on fitness (The higher the fitness, the greater the likelihood of selection).
- (Crossover) Crossover the parents to create new offspring (children) with a crossover probability. If there was no crossover, the children are identical replicas of their parents.
- (Mutation) Generate new offspring at each locus (chromosomal location) based on a mutation probability.
- (Acknowledging) Add additional progeny to the existing population.
- (Replace) For an additional algorithmic sum, use a newly produced population.
- (Test) Stop and return the best solution for the present population if the end condition is met.
- (Loop) Proceed to step 2 to assess your fitness.

GA is inefficient at locating local optima and is dependent on parallelism. PSO is favored in our situation

since it is difficult to establish the precise global optimum. GA is less effective than PSO at resolving identical issues. The idea of the suggested antenna is built on the usage of a circular patch with U slot into the radiating element. Using a FR-4 substrate with a 0.025 loss tangent and a 4.3 dielectric constant, the antenna is printed as shown in Fig. 2. The size of antenna element is 8.625 × 13.04 mm2. The radius of the circular antenna is determined by Equations (3) and (4) [5]. In the design, the height of substrate is h, the relative permittivity is εr, speed of light (3 × 108 m/s) is C and fr is the center frequency. The antenna's impedance is coordinated to 50 Ω and it spans the 26–40 GHz frequency range, while the antenna element's branching network's impedance is matched to 100 Ω. The gain of the proposed element and the radiation efficiency are at least 9dBi and 91%, respectively. The antenna covers the band of 5G mm Wave as shown in Fig. 3 (a). The dimensions of antenna using PSO are 13× 8.63 × 1.6 mm3 while the dimensions of antenna using GA are 13.71 × 8.46 × 1.6 mm3. The final parameters of the antenna element produced by PSO in CST and produced by GA are presented at Table 1. The PSO is used to decrease the design time, since it depends on few parameters and is easy to be constructed. PSO in CST takes the initial dimensions and the required fitness function and runs to get the final dimensions. The optimization aims are to obtain the smallest dimensions of the antenna in the essential bandwidth while achieving the fitness function [38-42]. The target in PSO (fitness function) is to have |S11| less than -10dB within the required bandwidth.

$$r = \frac{K}{[1+\frac{2h}{\pi F \epsilon_r}(\ln\{\frac{\pi F}{2h}\}+1.7726)]^{0.5}} \quad (3)$$

$$K = \frac{8.791*10^9}{f_r} \quad (4)$$

Tables 2 provides a summary comparison between the antenna parameters using the two optimization methods. According to Fig. 3 (b), the antenna's efficiency by PSO and GA is 91% and 89%, separately. Fig. 3 (c) shows the antenna's gain values according to PSO and GA which are 9 and 8.5 dBi, respectively. Figure 4 indicates the relevant current distribution for the suggested antenna element with numerous currents move in different directions. Fig. 5 (a) and (b) illustrate the simulated two-dimensional beam form at frequencies of 28 GHz and 38 GHz with Θ= 90° while Fig. 5 (c) and (d) are the 3D beam shaping for the antenna at 33GHz using PSO and GA, respectively. Due to theses currents, an increase in the operating bandwidth of antenna is noticed as shown in Fig. 6 (a). Combining these currents will consequently result in an improvement in bandwidth. The feeding line and borders of the circular antenna are where the majority of the flowing current is deposited.

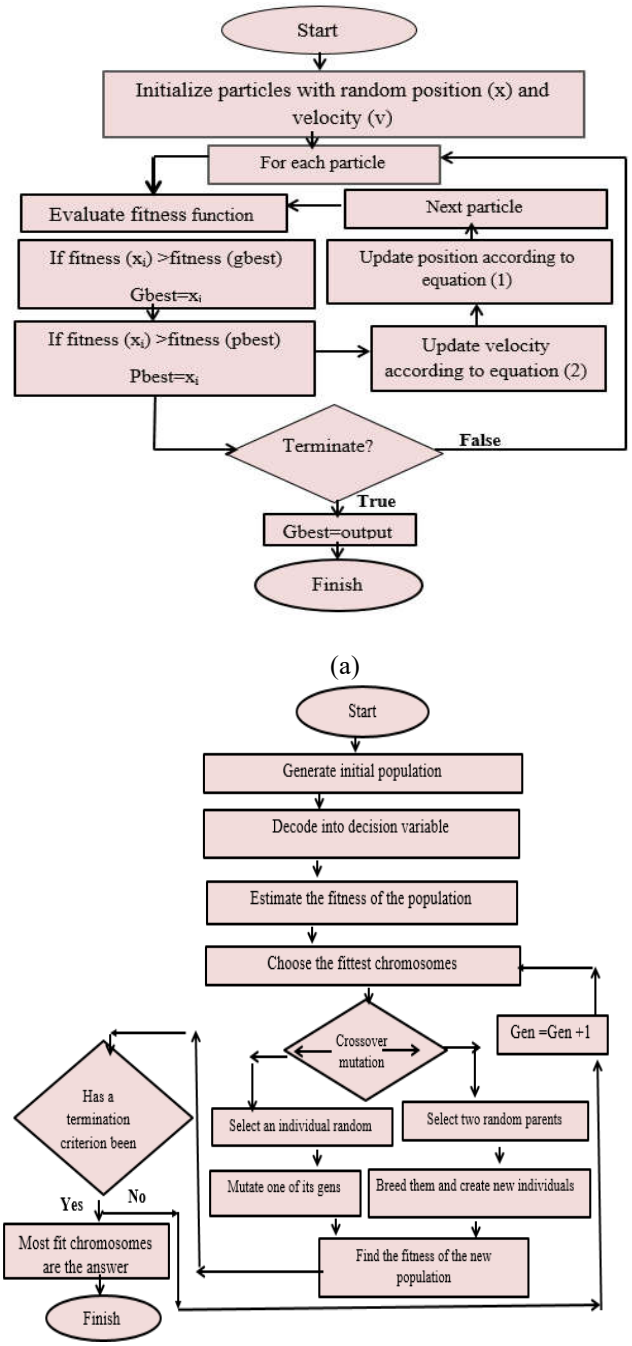

Figure 1: Flow chart of (a) PSO and (b)GA

The antenna is of 50Ω impedance and spans the 26–40 GHz spectrum while the impedance of the branched network in antenna element is 100 Ω. Fig. 6 (b) illustrates the impedance, which is 50 ohms. The antenna element beam shaping using the two algorithms are shown in Table 3 and Table 4. The dimensions of each element are 8.625, 13.04, 1.6 mm, respectively.

A "U" slot is injected through the antenna. The MIMO system is divided into two circular patch array elements, each of which is made up of a 1×2 array on a partly ground plane. A separation of 0. 5 λ, where λ is the

working wavelength, is chosen between each two adjacent elements.

The design process of the antenna element depends on Particle Swarm Optimization (PSO) and Genetic Algorithm (GA) with initial weight equals to 1 and with initial dimensions that result from the equations 1 and 2. PSO and GA in CST simulator takes the initial dimensions and the required fitness function and runs to get the final dimensions. MIMO array is constructed from the element based on PSO as it requires few parameters and is easy to construct.

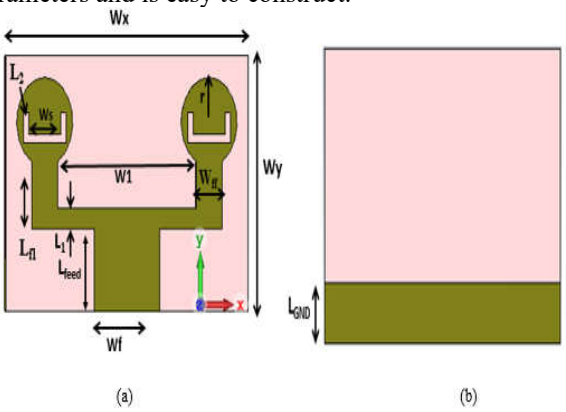

Figure 2: Geometry of proposed antenna; (a) Front side and (b) Backside

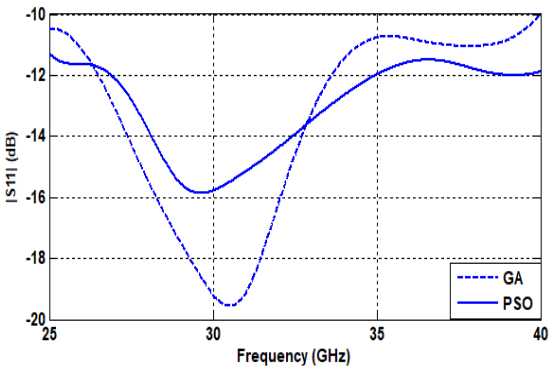

(a)

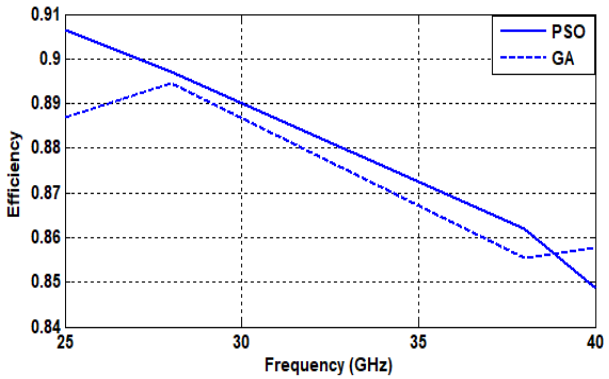

(b)

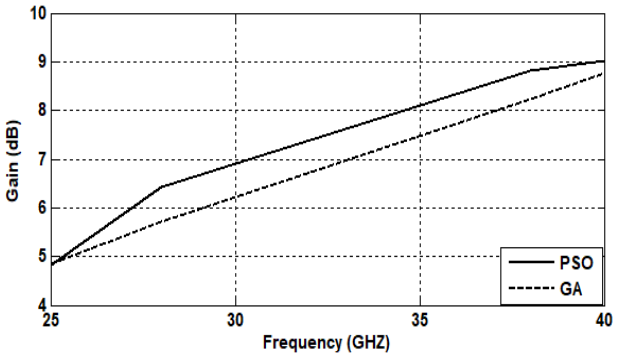

(c)

Figure 3: (a) Return Loss of the antenna using PSO and GA against the frequency, (b) Efficiency and (c) Gain

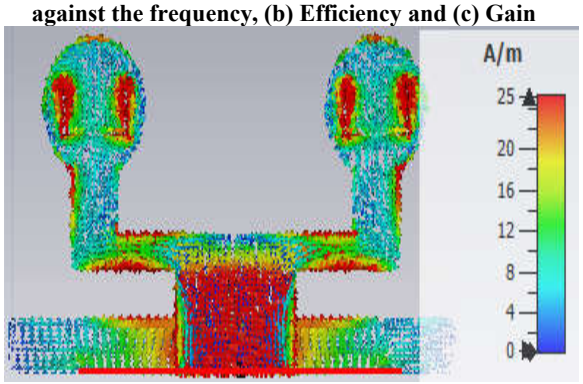

(a)

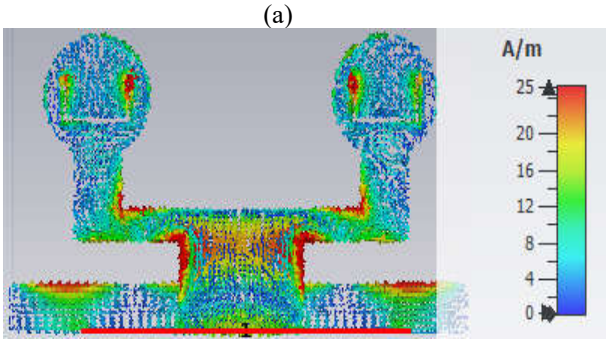

(b)

Figure 4: Antenna current density at frequencies; (a) 28 GHz and (b) 38 GHz

Table 1. Antenna element dimensions using PSO and GA (in Millimeters).

Parameters	GA	PSO
Wx	13.71	13
Wy	8.46	8.63
L_{feed}	2.37	2.78
L_1	0.6	0.68
W_f	3.485	3.485
W_1	7.41	7.41
W_{ff}	1.26	1.43
L_{GND}	1.1	1.76
L_{f1}	2.36	2.4
r	1.5	1.51
Ws	1.65	1.69
L_2	0.27	0.3

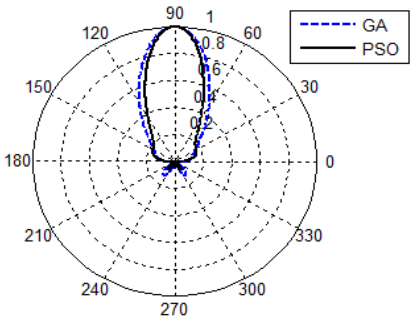

(a)

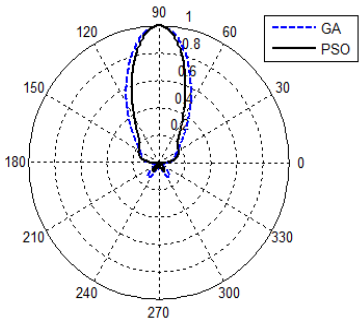

(b)

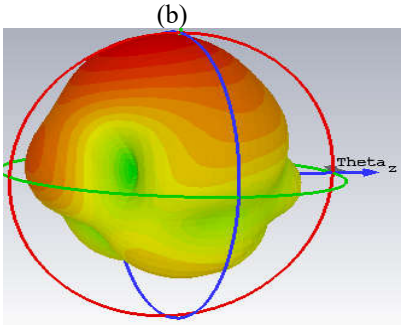

(c)

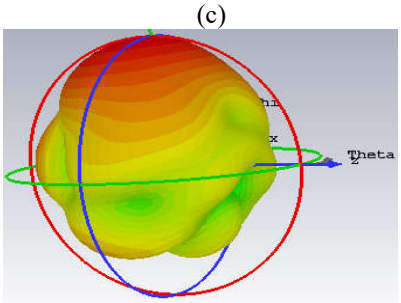

(d)

Figure 5: Beam-shape of antenna element at Θ =90° aimed at the frequencies of (a) 28 GHz, (b) 38 GHz and 3D beam forming at 33 GHz, (c) PSO and (d) GA

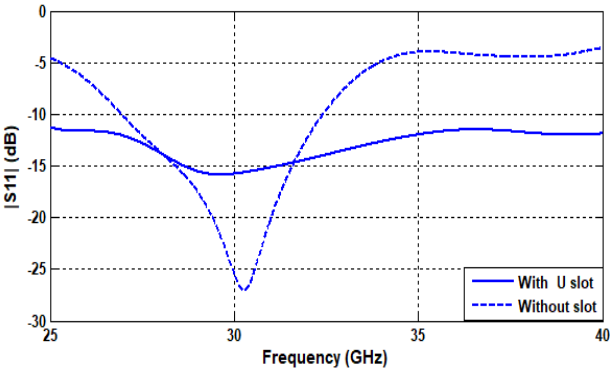

(a)

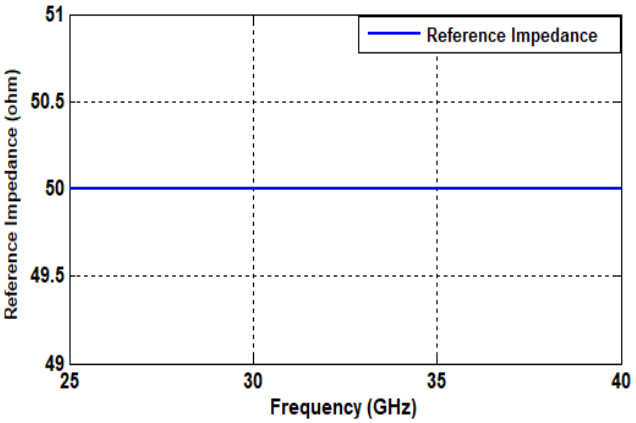

(b)

Figure 6: (a) Reflection Coefficient of the antenna using PSO with U slot and (b) Reference impedance of antenna

Table 2. Comparison summary between the two optimization techniques (PSO and GA).

	Optimization techniques	
	GA	PSO
No of Iterations	17	5
Speed	Medium	Fast
Complexity	Complicated	Simple-easy
BW	25- 40GHz	25- 40GHz
Efficiency	Greater than 90%	≈ 90%
Gain	8.5dB	9dB
Accuracy	Lower than PSO	larger
Design dimensions	13.71 × 8.46 × 1.6mm^3	13 × 8.63 × 1.6mm^3

Table 3. Outcomes of the considered two antenna's beam-forming using the method of (PSO).

Freq (GHz)	Parameters at Θ=90° plane			Parameters at Φ=0° plane		
	HPBW	MLM (dBi)	SLL (dB)	HPBW	MLM (dBi)	SLL (dB)
28	56.4°	4.59	-2.5	56.4°	5.2	-5
33	62°	5.31	-5.2	74°	6.72	-5.7
38	58.7°	8.27	-8.7	58.7°	8.38	-4

Table 4. Outcomes of the considered two antenna's beam-forming using the method of (GA).

Freq (GHz)	Parameters at Θ=90° plane			Parameters at Φ=0° plane		
	HPBW	MLM (dBi)	SLL (dB)	HPBW	MLM (dBi)	SLL (dB)
28	52.6°	5.52	-3.5	42.6°	8.85	-6.9
33	97°	5.59	-6	46.3°	7.05	-4
38	54.8°	9.29	-6.4	53.2°	9.13	-11

HPBW: Half Power Beam Width, MLM: Main Lobe Magnitude, SLL: Side Lobe Level.

3 TWO -PORT MIMO ARRAY ARCHITECTURE

FR-4 is used as the substrate for the intended antenna array. The recommended antenna array seen in Fig. 7 is simulated by the CST Microwave Studio 2019 software. The National Telecommunications Institute (NTI) in Egypt tests the design once it is constructed as illustrated in Fig. 8. The antenna array's total dimensions are 25.4 × 15.45 × 1.6 mm^3. The operational wavelength is represented by λ, and the indicated spacing between antenna elements is 0.5 λ.

4 RESULTS AND DISCUSSION

The intended array, Figs. 7 and 8, has a bandwidth of 27 to 40 GHz to handle 5G millimeter wave applications, particularly at 28 and 38 GHz, as seen in Fig. 9 (a). To mitigate the reciprocal coupling between ports, the design is comprised of two orthogonal parts, as shown in Figure 7. Inserting two transmission lines, each with a thickness of 0.2 mm to act as a capacitive element with dimensions (X1 = 6 mm, X2 = 8 mm, and X3 = 0.6 mm) between elements increases the isolation between ports to more than −30 dB, as demonstrated in Fig. 9(b). Fig. 9 (c) displays the isolation between elements in the absence of a decoupling element. The maximum efficiency and gain, which are approximately 93% and 10 dBi, correspondingly can be seen in Figs. 10(a) and (b). A possible explanation for the little discrepancy between the simulated and experimental findings could be the soldering of the SMA connector. In the meanwhile, the variation is still within the permitted range. Fig. 11 displays the surface current at 33 GHz when port 2 is in use.

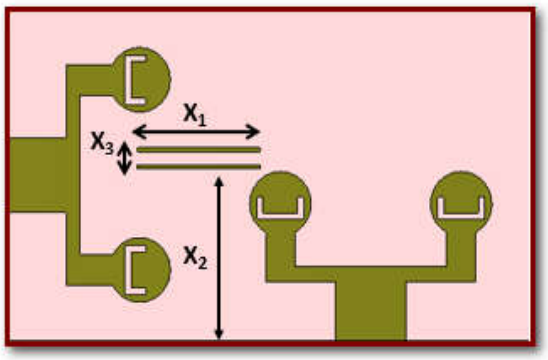

(a)

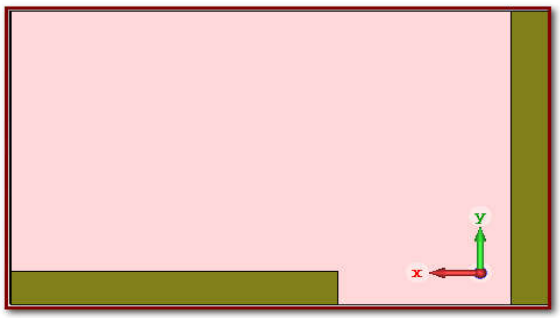

(b)

Figure 7: Two-port array; (a) Front side and (b) Backside

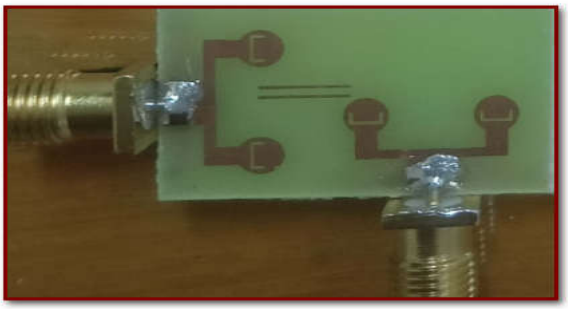

(a)

(b)

Figure 8: Suggested antenna fabrication; (a) Front side and (b) Back side

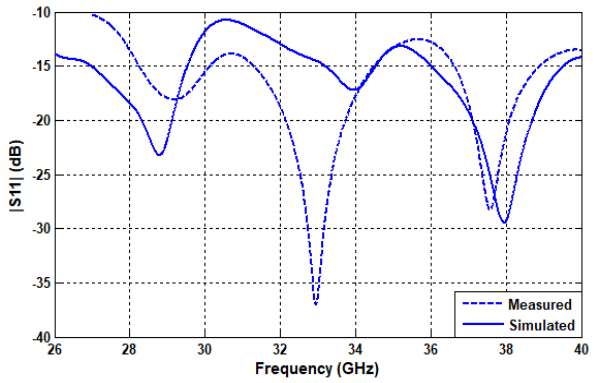

(a)

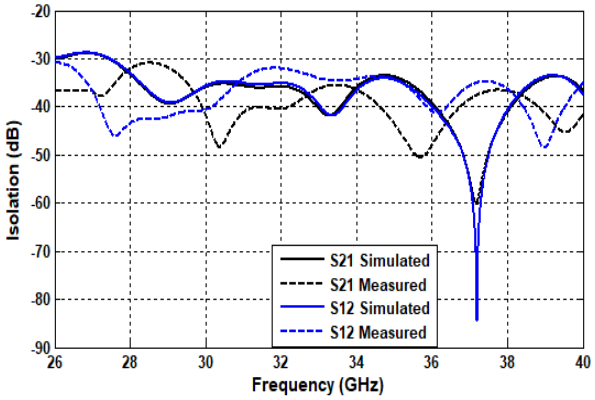

(b)

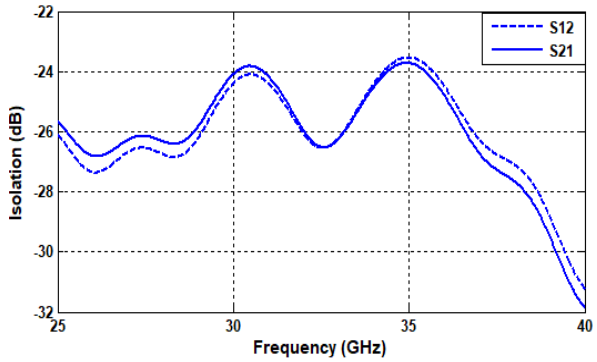

(c)

Figure 9: (a) Reflection coefficient at port 1, (b) Isolation between output ports after inserting capacitive element; and (c) Simulation of isolation between output ports without capacitive element

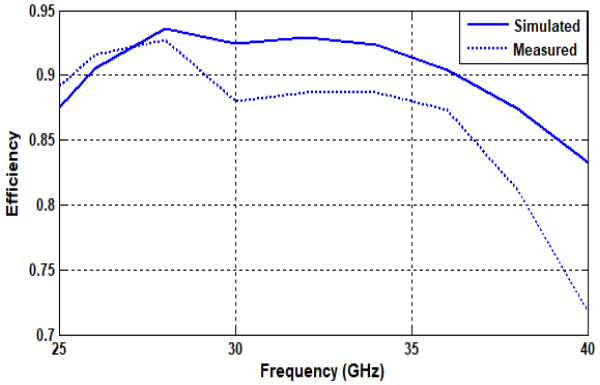

(a)

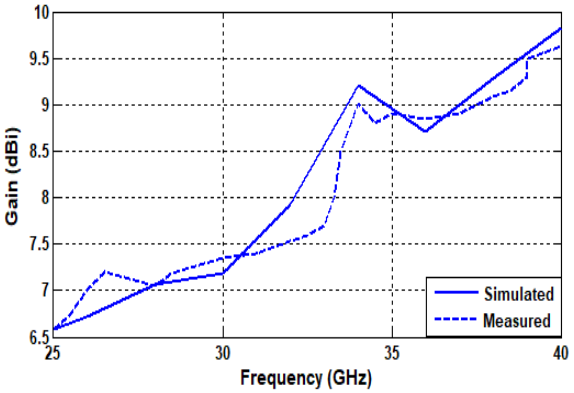

(b)

Figure 10: (a) efficiency, and (b) gain over frequencies

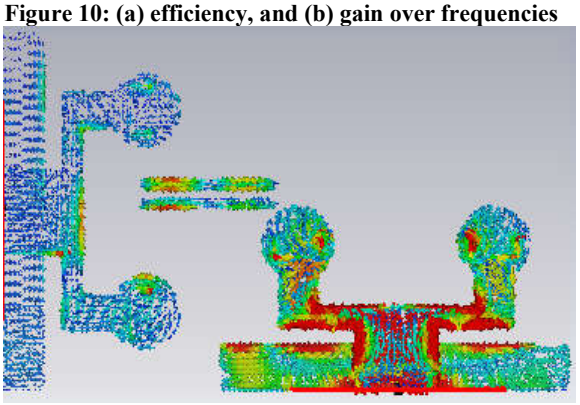

(a)

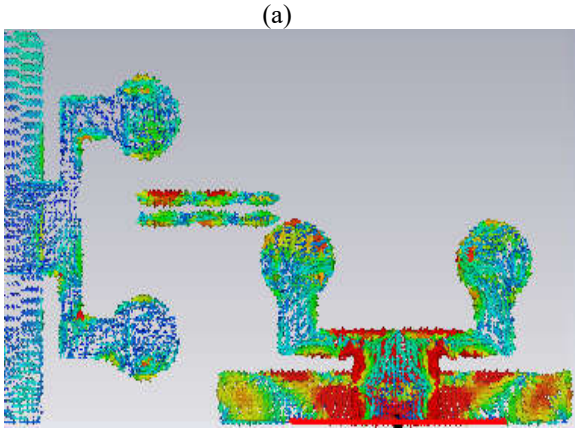

(b)

Figure 11: Current spreading when port1 is on (a) at frequency=28GHz and (b) at frequency=38HZ

The E-plane radiation shape for frequencies of 28 GHz and 38 GHz is displayed in Figure 12. As exposed in Figure 12(a), (b), (c), and (d), the main lobe is oriented at θ = 90°, and the beams at ports 1 and 2 are perpendicular to each other. The E-plane forms at X=90°, the beam is aimed at 180° with low Side Lobe Level (SLL) at port 2, and the greatest electric field is focused at θ=90° at port 1. The outcomes of the MIMO radiation parameters at 28 GHz, 33 GHz, and 38 GHz are exposed in Table 5.

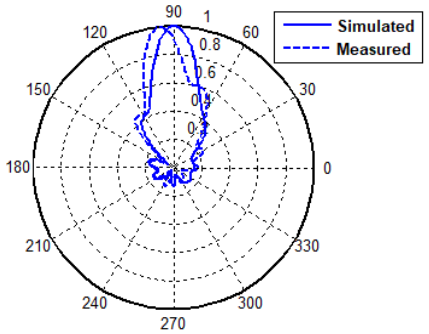

(a)

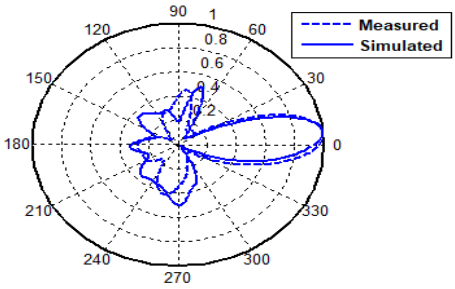

(b)

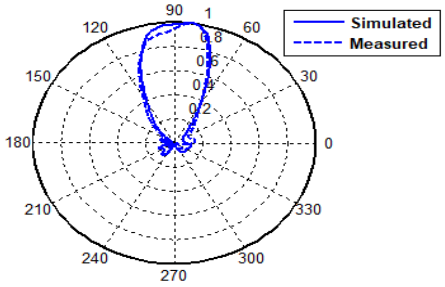

(c)

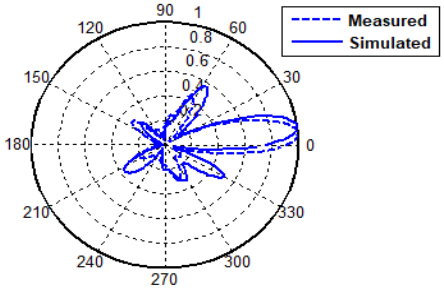

(d)

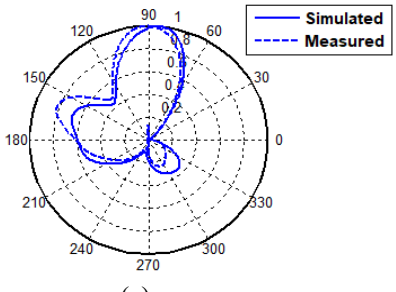

(e)

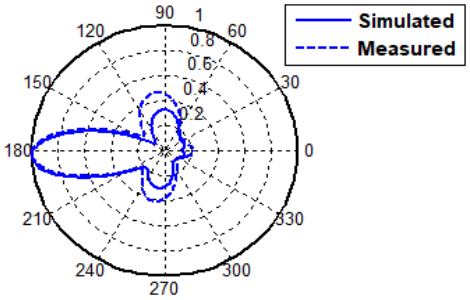

(f)

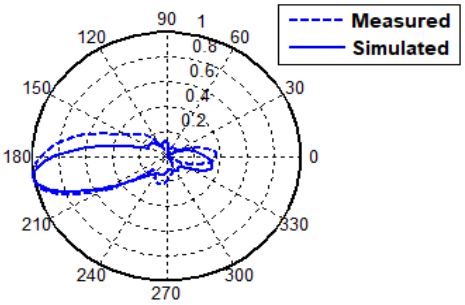

(g)

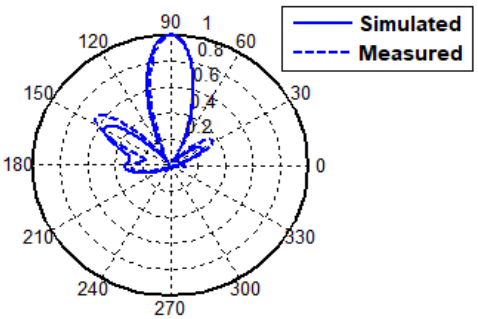

(h)

Figure 12: Beam pattern measured and simulated at θ =90º with 28GHz (a) Port1, (b) port2, with frequency of 38 GHz, (c) port1, (d) port2 and at Φ =90º; with frequency of 28GHz, (e) Port1, (f) port2, with frequency of 38 GHz, (g) port1 and (h) port2

Table 5. Beam forming outcomes of the MIMO.

Freq (GHz)	Θ=90º plane			Φ=90º plane		
	HPBW	MLM (dBi)	SLL (dB)	HPBW	MLM (dBi)	SLL (dB)
28	42.3º	6.81 dBi	-7.4	65º	6.81	-1 dB
33	51.9º	8.88 dBi	-8.7	40.2º	8.88	-4 dB
38	57.6º	9.44 dBi	-9.3	34.8º	8.67	-2 dB

5 EVALUATION PERFORMANCE OF MIMO ARRAY

A few parameters are utilized to examine the act of the MIMO array. Among these is the envelope correlation coefficient, or ECC. It's used to assess how well MIMO systems perform. The ECC [3] can be calculated depending on the radiation fields as shown in equation [5].

$$\rho_{mn}=\frac{\left|\iint_0^{4\pi}[\overrightarrow{F_m}(\Theta,\Phi)\times\overrightarrow{F_n}(\Theta,\Phi)]d\Omega\right|^2}{\iint_0^{4\pi}|\overrightarrow{F_m}(\Theta,\Phi)|^2\,d\Omega\iint_0^{4\pi}|\overrightarrow{F_n}(\Theta,\Phi)|^2\,d\Omega} \quad (5)$$

where ρ:ECC, $F(\Theta,\Phi)$: the antenna radiation patterns, $m\ or\ n$ are the number of the antenna.
The outcome of ECC is roughly < 2×10^{-4} as drawn in Fig.13a)

The Diversity Gain (DG) statistic is another parameter that measures transmission power loss in MIMO setups with diversity processes [6].

$$DG = 10\times(1-ECC^2)^{0.5} \quad (6)$$

DG is nearly 10 dB as offered in Fig. 13 (b).

(TARC) is the third component influencing port coupling. It is the relationship between the power released and the overall power incident. Equation 7 allows for an estimation, which is as follows [3]; $\Gamma = \left[\left(\left|S_{mm}+S_{mn}e^{j\theta}|^2\right)+\left(\left|S_{nm}+S_{nn}e^{j\theta}|^2\right)/2\right]^{0.5}$ (7)

S_{mm} and S_{nn} are the values of return loss for port 1 and port 2, respectivelly as seen in Fig. 13 (c).

The performance indicators channel capacity loss (CCL) is a very significant indication for evaluating systems that utilize MIMO. Utilizing the following equation, CCL is determined.

$$C\ loss = -\log_2(\Psi^R) \quad (8)$$

, in the previous equation, Ψ^R can be stated by the subsequent formula:

$$\Psi R = \begin{matrix}\Psi_{ii} & \Psi_{ij}\\ \Psi_{ji} & \Psi_{jj}\end{matrix} \quad (9)$$

Here, Ψ ii = 1 — ($|Sii|^2 + |Sij|^2$), Ψ ij= - ($Sii * Sij + Sji *$ Ψjj), Ψjj = - ($Sjj * Sji + Sij * Sii$),
Ψjj = 1 — ($|Sjj|^2 + |Sji^2$).

The wanted value of this parameter is to be ≤ 0.4 bits/s/Hz. In the suggested design, accordingly, it is achieved in Fig. 13 (d).

An extra parameter is the measured Mean Effective Gain (MEG), which assesses the antenna channel mismatched and takes into consideration total efficiency and gain.

The first antenna has a value of MEGi, and MEGj is for the second antenna. MEG values are listed in Table 6. It could be calculated from equations (10) and (11).

$$MEGi=0.5(1-|Sii|^2-|Sij|^2) \quad (10)$$

$$MEGj=0.5(1-|Sji|^2-|Sjj|^2) \quad (11)$$

The proposed equivalent circuit of the considered two port MIMO system is obtainable in Fig.14. The equivalent circuit is signified by inductance (Lp), resistance (Rp which equals to 50Ω for matching), and capacitance (Cp). Cp and Lp are responsible for electric and magnetic coupling between the antenna elements, separately. Due to the small distance between antennas, the problem of mutual coupling appears. In order to reduce the mutual coupling, A capacitive element (R_{Ds}, L_{Ds}, C_{Ds}) is inserted between the antennas. As Capacitive element add further capacitance that makes more isolation between elements and it can make a satisfactory quantity of decoupling current and advance isolation [3].

Table 7 introduces a comparison between the performance of the previous studies and preceding work. The proposed MIMO antenna array operates within a broad band 26-40GHz with high gain of 10dBi and %93 efficiency. A capacitive element between antennas affords excellent isolation at 37.5 GHz (-85 dB) and enhances MIMO capability for DG, CCL, ECC, TARC, and MEG.

The antenna is fabricated from low-cost FR-4substrate material. Although the efficiency and isolation are higher in references [9], the size of the antenna is larger than the proposed design, the cost is more expensive as it is fabricated from (Rogers RO3003). In [5], the efficiency is higher than the efficiency of the proposed antenna also, but the size of the planned antenna is smaller and the substrate material and isolation are the same.

The consequences of the planned antenna are better than the others. Figure 15 illustrates the process and summarizes the steps of the proposed design for the two-port array. Table 8 presents a comparison between the performance of previous studies and preceding work with respect to the algorithms used in fabrication, taken time and number of trials.

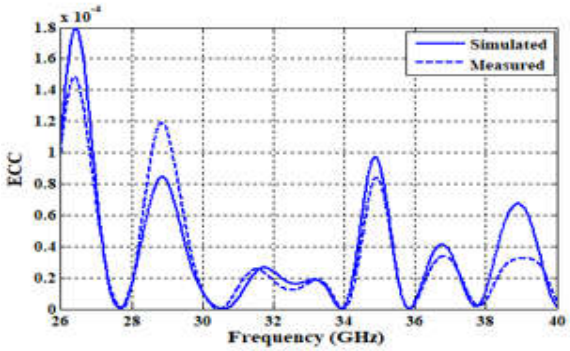

(a)

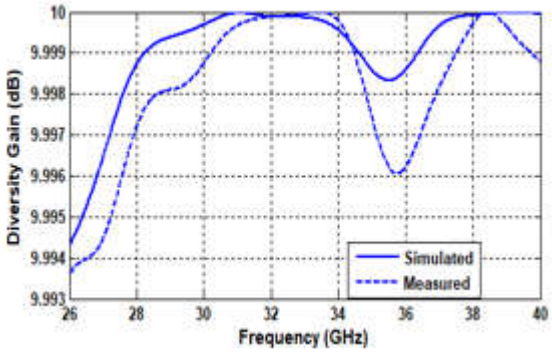

(b)

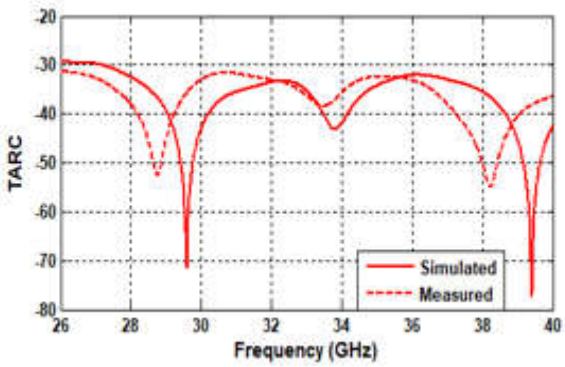

(c)

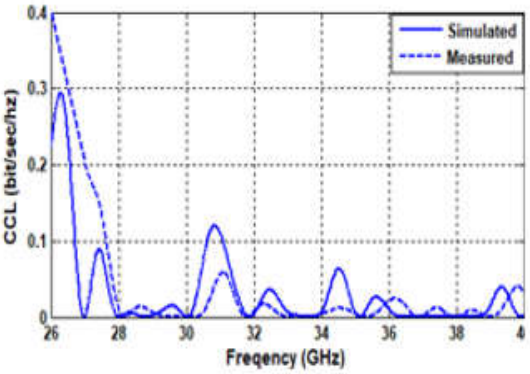

(d)

Figure 13: (a) ECC, (b) DG, (c) TARC and (d) CCL for the MIMO system

Table 6. MEG values at different frequencies for MIMO antenna system

Freq (GHz)	(MEG)		
	MEG1	MEG2	MEG1/ MEG2
28	−6.32	−6.02	0.97
33	−6.61	−6.55	0.99
38	−6.34	−6.41	1.01

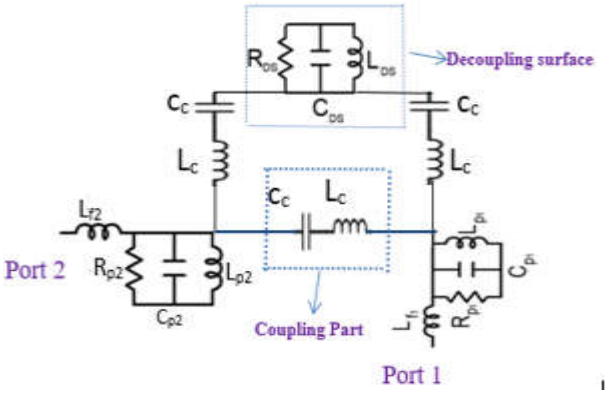

Figure 14: Proposed two port antenna arrays with capacitive element equivalent circuit

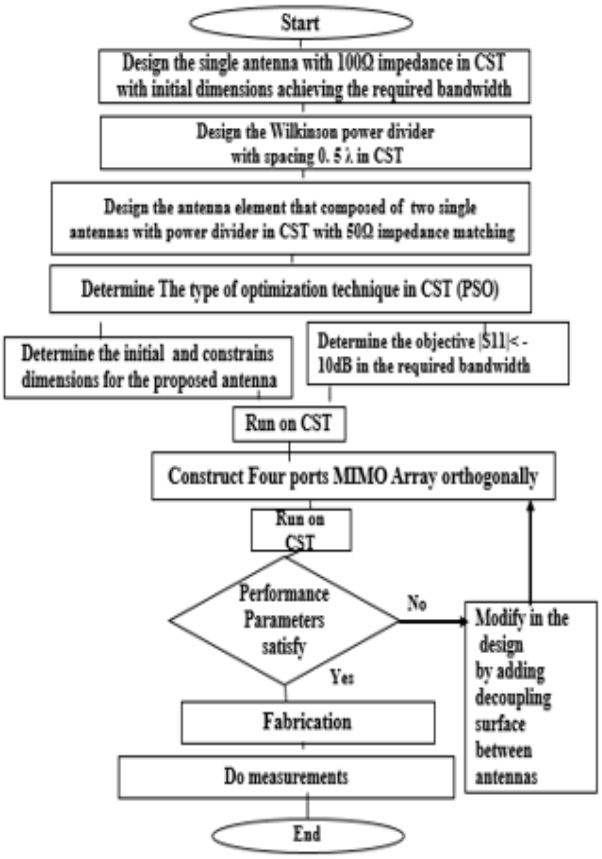

Figure 15: Flow chart of the proposed two port MIMO design

Table 7. Comparison between the performance of previous studies and preceding work.

Ref	No. of ports	Substrate	Profile antenna array	Coupling way	Isolation advance (dB)	Design difficulty	BW percentage GHz	Size mm^3	DG	CC	Gain dBi	Efficiency %
1]	8	FR4	0.019 λ	DGS	−12	Easy	22.22%	.78 λ× 0.89λ	NA	0.01	2.5	70
2]	4	Rogers RT/Duroid5880	0.047 λ	----------	−12	Easy	20%	.8 λ × 4.3 λ	NA	Not found	13.1	Not found
3]	4	FR4	0.023 λ	DGS-EBG-NL-PE	−25	Medium	62.5%	.46λ× 1.46λ	9.9	.05	9	90
4]	6	FR4	0.054 λ	Metamaterial photonic	-12	Easy	16%	4 λ ×1.4 λ	NA	Not found	7.38	88
5]	2	FR4	0.184 λ	Isolating element	−30	Easy	38.8%	6.1λ ×3 λ	10	10^{-4}	10	95
6]	4	Rogers R04350B	0.069 λ	DGS	-20	Medium	14.5%	2.75λ× 3.2 λ	>9.96	0.01	8.3	82
7]	8	Rogers 5880	0.0156 λ	NA	−20	Medium	7%	0.9λ×0.3λ	NA	Not found	9.3	NA
8]	4	Duroid 5880	0.086 λ	NA	-25	Medium	30.3%	4.6λ×0.88 λ	9.96	.004	5.5	84
9]	4	Rogers RO3003	0.027 λ	PE	-35	Easy	30.3%	16 λ × 8 λ	9.99	.0002	9	97
10]	4	Taconic TLY-5	0.055 λ	NA	-35	Medium	30%	0.7λ ×0.88 λ	NA	A	9	84
11]	4	FR4	0.046 λ	Metamaterial	-17	Medium	14.5%	.4λ ×2.6 λ	NA	As	7	88
14]	4	RO4350B	0.029 λ	double-layer meta-surface	−25	Difficult	10%	.12λ× 2.12λ	Not found	0.12	5	77
roposed design	2	FR4	0.176 λ	Orthogonality, decoupling surface	−30	Easy	42.42%	.7λ× 1.7λ	>9.994	0.002	10	93

Table 8. Comparison between the performance of previous studies and preceding work with respect to the algorithms used in fabrication, taken time and number of trials in addition to gain, efficiency, size and substrate.

Ref	Fabrication Algorithm Used	No. of Trials	Time-Taken (minutes)	Gain (dBi)	Efficiency	Size (mm^3)	Substrate
[3]	PSO	15	-	9	90%	1.46λ× 1.46 λ	FR-4
[23]	GA - MOM (Method of Moment)	200	50	-	-	1.7λ× 1.7λ	Rogers 5880
[24]	GA	50	-	7.6	-	0.77λ× 0.77λ	FR-4
[25]	GA	30	A few hours	6	90%	0.06λ × 0.428λ	RO4725JXR Ɛr=2.55
[26]	PSO	100	7	-	-	2.4λ× 2.4λ	Ɛr = 2.94
[27]	PSO	15	-	6	95%	1.2λ× 1.01λ	Roger RT5880
[28]	NN	1500	10	-	-	0.22λ× 0.23λ	Ɛr=4.5
[37]	GA-ANN	100	-	-	-	1.25λ× 0.67λ	Ɛr=4.5
Proposed design	GA- PSO	17-5	35-15	10	93%	2.7λ× 1.7λ	FR-4

6 CONCLUSION

A two-port MIMO array with great antenna separation is shown in this work. Two circular patch array elements make up the arrangement. Every component is made up of a 1x2 array of antennas. Antenna arrays provide the benefit of high gain. To increase bandwidth, a U-Slot is installed in each radiating element. The antenna model's improved-dimension element has been simulated using PSO and CST program. The isolation between ports can be improved to be less than -30dB by putting a decoupling surface in between the two ports. The recommended design is printed at a notably lower cost on a FR-4 substrate. An observed consistency between the measured and simulated outcomes is noted. In order to function in 5G mm Wave requests, the antenna functions in the 26–40 GHz frequency range. Besides, the TARC is < -25 dB and the ECC value is less than 0.0002, indicating strong CCL performance. The array offers a nearly 10-dBi gain and a high maximum efficiency of 93%. To design the antenna element, Particle Swarm Optimization is used.

Acknowledgments The authors would like to thank the respected editors and the reviewers for their helpful comments.

Author contributions A Conceptualization, A.A.M., and H.Y.S; methodology, A.A.M; software, H.Y.S.; validation, A.A.M.; formal analysis, H.Y.S. and A.A.M; investigation, H.Y.S. and A.A.M; resources, H.Y.S.; data curation, H.Y.S and A.A.M; writing—original draft preparation, A.A.M; writing—review and editing, H.Y.S.; visualization, H.Y.S.; supervision, H.Y.S. All authors have read and agreed to the published version of the manuscript.

Funding None

Data availability Data is contained within the article.

Declarations

Competing interests The authors declare no competing interests.

7 REFERENCES

[1] Naser Ojaroudi Parchin, Haleh Jahanbakhsh Basherlou, Mohammad Alibakhshikenari, Yasser Ojaroudi Parchin, Yasir I. A. Al-Yasir, Raed A. Abd-Alhameed, and Ernesto Limiti. "Mobile-Phone Antenna Array with Diamond-Ring Slot Elements for 5G Massive MIMO Systems," Electronics, vol. 8, no. 5, pp. 1- 17, 2019.https://doi.org/10.3390/electronics8050521.

[2] Nanae Yoon, Chulhun Seo. "A 28-GHz Wideband 2 × 2 U-Slot Patch Array Antenna," J. Electromagnetic Engineering and Science, vol. 17, no. 3, pp. 133-137, 2017.https://doi.org/10.5515/JKIEES.2017.17.3.133.

[3] Amany A. Megahed, Mohamed Abdelazim, Ehab H. Abdelhay, and Heba. Y. M. Soliman. "Sub-6 GHz Highly Isolated Wideband MIMO Antenna Arrays," IEEE Access (ISSN: 21693536), vol. 10, pp. 19875-19889, 2022. https://doi.org/10.1109/ACCESS.2022.3150278.

[4] Ayman A. Althuwayb. "Low-Interacted Multiple Antenna Systems Based on Metasurface-Inspired Isolation Approach for MIMO Applications," Arabian Journal for Science and Engineering, pp. 1-10, 2021. https://doi.org/10.1007/s13369-021-05720-6.

[5] Amany A. Megahed, Mohamed Abdelazim, Ehab H. Abdelhay, and Heba. Y. M. Soliman. "5G Millimeter Wave Wideband MIMO Antenna Arrays with High Isolation," EURASIP Journal on Wireless Communications and Networking, pp.1: 1-16, 2023. https://doi.org/10.1186/s13638-023-02267-y.

[6] Khalid, Mahnoor, et al., "4-Port MIMO antenna with defected ground structure for 5G Millimeter Wave Applications," Electronics, vol. 9, no. 1, pp. 1-13, 2020. https://doi.org/10.3390/electronics9010071.

[7] Fajar Wahyu Ardianto, Farhan Fathir Lanang, Setyawan Renaldy, and Trasma Yunita. "Design mimo antenna with U-Slot Rectangular Patch Array for 5G Applications," International Symposium on Antennas and Propagation (ISAP)., IEEE, pp. 241-242, 2018.

[8] U. Rafique, A. Shobit, N. Nasir, Kh. Hisham, and U. Khalil. "Inset-fed planar antenna Array for dual-band 5G MIMO applications," Prog. Electromagnet, Res. C., pp. 112: 83–98, 2021. https:// doi:10.2528/PIERC21021302.

[9] A.E. Farahat, and F.A.H. Khalid. "28/38 GHz dual-band Yagi-Uda antenna with corrugated radiator and enhanced reflectors for 5G MIMO antenna systems," Prog. Electromagnet. Res. C., pp. 159–172, 2020.https://doi:10.2528/PIERC20022603.

[10] P. Liu, W.Z. Xiao, Z. Yan, W. Xiang, Y. Chunfeng, and H.J. Zhi. "Patch antenna loaded with paired shorting pins and H-Shaped slot for 28/38 GHz dual-band MIMO applications," IEEE Access, vol. 8, pp. 23705–23712, 2020.https://doi: 10.1109/ACCESS.2020.2964721.

[11] C. Zebiri, M.L. Bouknia, D. Sayad, I. Elfergani, Moustafa H. Aly, Preecha Yupapin, Sarawoot Boonkirdram, Arpan Desai, and J. Rodriguez. "Gyrotropic reciprocal bianisotropic metamaterial printed dipole antenna: investigation of negative input impedance and mutual coupling," Alex. Eng. J., vol. 61, pp. 11677–11685, 2022. https:// doi.org/10.1016/j.aej.2022.05.012 1110-0168.

[12] W. Wu, B. Yuan, A. Wu. "A quad-element UWB-MIMO antenna with band-notch and reduced mutual coupling based on EBG structures," Int. J. Antennas Propag, pp. 1-10, 2018. https://doi.org/10.1155/2018/8490740.

[13] S. Roy, U. Chakraborty. "Mutual coupling reduction in a multi-band MIMO antenna using meta-inspired decoupling network," Wireless. Pers, Communication, vol. 114, no. 4, pp. 3231–3246, 2020.

[14] JIAZHI TANG, FAIZAN FARAZ, XIAOMING CHEN, QINGQING ZHANG1, QINLONG LI, YINGSONG LI, and SHUAI ZHANG. "A metasurface superstrate for mutual coupling reduction of large antenna arrays," IEEE Access, vol. 8, pp. 126859-126867, 2020.

[15] A. Birwal, S. Singh, B.K. Kanaujia, S. Kumar. "MIMO/diversity antenna with neutralization line for WLAN applications," MAPAN, vol. 36, pp. 763–772, 2021.

[16] S. Zhang, G.F. Pedersen. "Mutual coupling reduction for UWB MIMO antennas with a wideband neutralization line," IEEE Antennas Wireless Propag., Lett. Vol.15, pp.166–169, 2016.

[17] R.S. Ayman, A.E.A. Wael, and A.I. Ahmed. "Minimally coupled two-element MIMO antenna with dual band (28/38 GHz) for 5G wireless communications," J. Infrared Millimeter Terahertz Waves, vol. (43), pp. 335–348, 2022. https://doi.org/10.1007/s10762- 022-00857-3.

[18] L. D. Orazio. "Study and development of novel techniques for PHY layer optimization of smart terminals in the context of next generation mobile communications," University of Trento, Trento, Italy, 2008.

[19] Hafiz Usman Tahseen, Luciano Mescia, and Luca Catarinucci. "A survey of five generations of MIMO multiband base station antennas," Radio Science, vol. **58** e2023RS007725 (7), pp. 1-17, 2023. https://doi.org/10.1029/2023RS007725.

[20] Tahseen, Hafiz Usman, Zhaowen Zheng, and Lixia Yang. "A Single Substrate 38 GHz Dual Antenna Array with Compact Feed Network," IEEJ Transactions on Electrical and Electronic Engineering, vol. 16, no. 9, pp. 1203-1208, 2021.

[21] Nizar S, Anouar B, Islem BH, and Lassaad L. "Millimetre-wave dual-band MIMO antennas for 5G wireless applications," J Infrared Millim Terahertz Waves, vol. 44, pp. 297–312, 2023. https://doi.org/10.1007/s10762-023-00914-5.

[22] Soumik D, Sukomal D, and Shiban KK. "Isolation improvement of MIMO antenna using novel EBG and hair-pin shaped DGS at 5G millimeter wave band," IEEE Access, vol. 9, pp.162820–34, 2021. https://doi.org/10.1109/ACCESS.2021.3133324.

[23] J. Michael, and Yahya Rahmat-Samii. "Genetic algorithms and method of moments (GA/MOM) for the design of integrated antennas," IEEE Transactions on Antennas and Propagation, vol. 47, no. 10, pp. 1606-1614, 1999.

[24] Tung, Lam Vu, Nam Ha-Van, and Chulhun Seo. "A novel metamaterial design using genetic Algorithm for high gain energy harvesting antenna," IEEE wireless power transfer conference (WPTC). IEEE, pp. 123-126, 2020. https://doi: 10.1109/WPTC48563.2020.9295587.

[25] Derbal, Mohammed Cherif, Abdelbaki Zeghdoud, and Mourad Nedil. "A dual band notched UWB antenna with optimized DGS using genetic

algorithm," Progress, In Electromagnetics Research Letters, vol. 88, pp. 89-95, 2020.

[26] Jin, N., Rahmat-Samii, Y. "Particle swarm optimization for antenna designs in engineering electromagnetics," Journal of Artificial evolution and applications, vol.1, 2008. https://doi.org/10.1155/2008/728929.

[27] Elabd, Rania Hamdy, and Ahmed Jamal Abdullah Al-Gburi. "Design and Optimization of a Circular Ring-Shaped UWB Fractal Antenna for Wireless Multi-Band Applications Using Particle Swarm Optimization," Progress in Electromagnetics Research B 106 .2024. . https://doi.org/10.2528/PIERB24033002.

[28] VILOVIĆ, Ivan; BURUM, Nikša; BRAILO, Marijan. "Microstrip antenna design using neural networks optimized by PSO," In: ICECom 2013. IEEE, pp. 1-4, 2013. https://doi.org/10.1109/ICECom.2013.6684759.

[29] E. J. Wilkinson. "An n-Way Hybrid Power Divider,"IRE Trans, Microwave Theory Tech, vol. 8, pp. 116– 118, 1960.

[30] Taufiq qrrachman, Denipermana Kurniadi. "Design and Realization Wilkinson Power Divider at Frequency 2400MHz for Radar S-Band," Electronics and Communication En-gineering (IOSR- JECE), vol. 3, pp. 269- 30, 2012.

[31] Mohamed S. El-gendy, Haythem H. Abdullah, Esmat A. Aballah and Hadia M. El-Hennawy. "Compact Microstrip Feeding Network for Mobile Base Station Antenna," International Journal of Engineering Research, vol. 5, no. 7, pp. 567-571, 2016. https://doi:10.17950/ijer/v5s7/704.

[32] Moniruzzaman, M., Islam, M. R., Sopian, K., & Zaidi, S. H. "Antenna Design Using Particle Swarm Optimization," International Journal of Electromagnetism and Applications, vol. 2, no. 1, pp. 17-22, 2011.

[33] Hussein, M. K. "Design Microstrip Antenna Using Particle Swarm Optimization," Journal of Wasit for Science and Medicine, vol. 4, no. 2, pp. 162-173, 2011. https://doi.org/10.31185/jwsm.160.

[34] Fan, X., Y. Tian, and Y. Zhao. "Optimal design of multiband microstrip antennas by self-renewing fitness estimation of particle swarm optimization algorithm," International Journal of Antennas and Propagation, pp. 1–9, 2019. https://doi.org/10.1155/2019/2176518.

[35] Weile, D. S. and E. Michielssen. "Genetic algorithm optimization applied to electromagnetics: A review," IEEE Trans. Antennas Propag, vol. 45, no.3, pp. 343-353, 1997. https://doi:10.1109/8.558650.

[36] Milan Polivka, Milan Drahovzal, Jan Rohan, Pavel Hazdra. ". Multiband patch antenna with perturbation elements generated by genetic algorithm," Proc. 'EuCAP 2006, pp. 6-10, 2006.

[37] KAUR, Gagandeep; RATTAN, Munish; JAIN, Chahat. "Design and optimization of psi (ψ) slotted fractal antenna using ANN and GA for multiband applications," Wireless Personal Communications, vol. 97, pp. 4573-4585, 2017.